ifas Institute for Fluid Power Drives and Systems | RWTH AACHEN UNIVERSITY

11!FK 11!FK

Global Fluid Power Society

hp

VDMA

GENERAL

Matthias Petry

+49 (0) 241 - 80 47 733
general@ifk2018.com

TRADE EXHIBITION

Jutta Zacharias

+49 (0) 241 - 80 47 711
exhibition@ifk2018.com

CONTRIBUTORS

Stephan Merkelbach

+49 (0) 241 - 80 47 722
papers@ifk2018.com

ADDRESS

Campus-Boulevard 30
D-52074 Aachen

+49 (0) 241 - 80 47 711
+49 (0) 241 - 80 6 47 712
post@ifas.rwth-aachen.de
www.ifas.rwth-aachen.de

11TH IFK | CONFERENCE PROCEEDINGS

FLUID POWER NETWORKS

19th - 21st MARCH 2018 | PROCEEDINGS

11TH INTERNATIONAL FLUID POWER CONFERENCE

Vol. 3

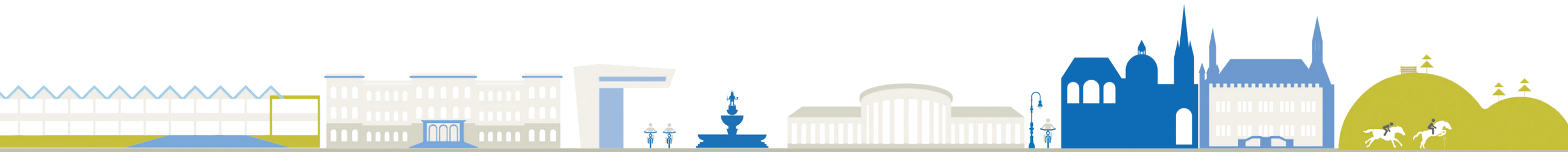

Disordered flow to the reservoir – measures to improve the situation

Baum, Heiko* and Scheffel, Gerd**

FLUIDON GmbH, Jülicher Str. 338A, 52070 Aachen*
heiko.baum@fluidon.com
Parker Hannifin GmbH, Gutenbergstr. 38, 41564 Kaarst**

To reduce cycle times, hydraulic drives become consciously more dynamic, what consequently leads to higher fluid exchange rates. On the part of the pressure supply no effort is too big for the design engineers. The return pipe to the tank is, however, often still calculated with rough formulas. This can lead to damages to the plant by cavitation, water hammers and diesel effects and is no longer up-to-date.

On investigating water hammer events in tank-pipes it becomes obvious that an examination with simple rough calculations is not leading to the desired results. Too many factors must be considered at the calculation of water hammer. Fortunately, nowadays the numeric simulation can calculate the pressure gradient and the pressure amplitude of a water hammer in very good approximation. Thus, by means of simulation a basic understanding of the problem in the tank pipe can be achieved.

In this contribution the boundary conditions which lead to the emergence of a water hammer after cavitation are introduced. Calculation examples explain the differences of water hammers in drives with HLP fluid and with HFC fluid. By the combination of the simulation results to nomograms, a practice-fit tool is introduced, which can be used to assess the water hammer vulnerability of a drive already during the project planning. The presentation of possible constructive remedial measures completes this contribution.

Keywords: water hammer, cavitation, column separation, tank pipe, simulation
Target audience: Design Process, Simulation

1 Introduction

One often only thinks of water hammer at rapid flow changes in supply pipes. However, water hammer in return pipes to the tank much more frequently occurs when the speed of the fluid is braked down to standstill. Unlike the water hammer in supply pipes a short but decisive time period is passed through with a very low pressure at the water hammer in tank pipes, though.. The cause of the low pressure is the inductance of the fluid column. Kinetic energy, stored in the moving fluid column, must be reduced by a braking pressure difference before the fluid column stops. Through the braking pressure the fluid column is then accelerated back towards the entrance of the tank pipe by what the water hammer is started.

At the analysis of water hammers it must be considered that hydraulic systems use different fluids. While most hydraulic plants use a mineral oil based fluid (e.g. HLP) as an operation medium there are also heavily inflammable fluids (e.g. HFC) for use in pressure die casting machines. The fluid properties of HLP and HFC (**Figure 1**) are, however, considerably different, what in turn influences the events during the mentioned period of low pressure.

What exactly happens in the fluid during the deceleration process depends, in addition to the fluid properties, also on the air content of the fluid. Here the dissolved as well as the undissolved air must be considered. Depending on the velocity of the fluid, the braking pressure and the turnoff-time of the flow (e. g. valve closing time), a pseudo cavitation zone will develop with HLP whereas with HFC there will be real cavitation. In any case, during the braking process there will be a development of bubbles that contain a fluid steam air mixture.

Fluid	HLP	HFC	Water
Density at 15 °C [kg/m³]	0.86	1.04 – 1.09	1
Kinematic viscosity at 40°C [mm²/s]	46	46	0.658
Bulk modulus [N/m²]	2.0×10^9	3.5×10^9	2.14×10^9
Recommended temperature range [°C]	-10 – 100	-20 – 60	n. a.
Flash point [°C]	ca. 220	n. a.	n. a.
Ignition temperature [°C]	310 – 360	none	none
Bunsen coefficient for air at 20 °C	0.08 – 0.09	0.01 – 0.02	< 0.02
Speed of sound at 20 °C [m/s]	1,300	ca. 1,400	1,480
Vapor pressure at 50 °C [mbar]	10^{-4} / 10^{-5}	ca. 50 - 80	123
Danger of cavitation	Low	average	high

Figure 1: Water hammer relevant fluid parameter for HLP, HFC (excerpt of a table from /1/) and water

The fluid column streaming back at first “fills up” the area of low pressure at the start of the tank pipe, constantly accelerated be the braking pressure. If the fluid column then comes to a stop the water hammer occurs accompanied by the structural shock that damages the system mechanically. The high pressure amplitudes during the so called *Joukowsky* impact /2/ also compress the fluid steam air mixture bubbles and produce high temperature inside the bubbles. In mineral oil systems it now comes to the diesel effect and the fluid steam air mixture ignites. For plants with HFC this leads to thermal damages by the hot bubbles. The exact physical courses of the formation of bubbles are still not known completely. One knows today, however, that the composition of the fluid steam air mixture, the temperature level in the bubble and the pressure gradient are essential influence variables /3, 4, 5/. A survey about the fluid property dependent distinction of water hammer events in hydraulic drives with HLP and HFC fluid is given in by *Baum* and *Scheffel* /6, 7/. Complementary literature about the influence of dissolved air and of undissolved air onto the dynamics of fluid power systems is given by *Murrenhoff* and *Schmitz* /8, 9/.

It must be the aim of the plant design to avoid critical pressure gradients at the important operation points of the system. Due to the numerous influence factors, such a design is no longer possible with rough formulas, though. By means of simulation, an automated analysis of the deceleration process would help to understand the dynamic events during the deceleration process system-specifically and would support the conception of remedial measures to avoid water hammer events.

2 Pipe model for water hammer simulation

It is important to the simulation of a water hammer that besides the actual pressure blow the used pipe model also considers the "past history", that are the cavitation or the pseudo cavitation like conditions in the tank pipe.

The pipe model in DSHplus /10/ is based on the method of characteristics (MOC) whose suitability for water hammer simulation is extensively discussed by *Mambretti* /11/. At the RWTH Aachen this method was first used by *Theissen* /12/ for the simulation of hydraulic piping and later was extended by *Müller* /13/ for pipes with viscoelastic material behaviour of the pipe wall. Both model variants already contained approaches to calculate the frequency dependent friction, that, however, were limited to laminar flow conditions. The model used for the simulations is extended by a frequency dependent friction calculation according to *Vardy & Brown* /14/ and is, under consideration of the relative wall roughness, valid for turbulent flows at very high Reynolds numbers.

The consideration of the cavitation is taken from numeric approaches from water hydraulic systems which can be integrated very well into the MOC procedure. A paper of *Bergant* /15/ delivers a comprehensive overview over "Water hammer with column separation". The pipe simulation model, currently available in DSHplus, already considers pressure dependent fluid parameter. Thus, a two-phase model, such as described by Neuhaus /16/ as “3 equation model”, could be selected for the cavitation calculation. The two-phase model can handle bubble flows, that either develop due to outgassing of air from the fluid or develop from fluid steam air mixture in a pseudo cavitation zone. Moreover, the two-phase model can cover short-duration pressure peaks (**Figure 2**).

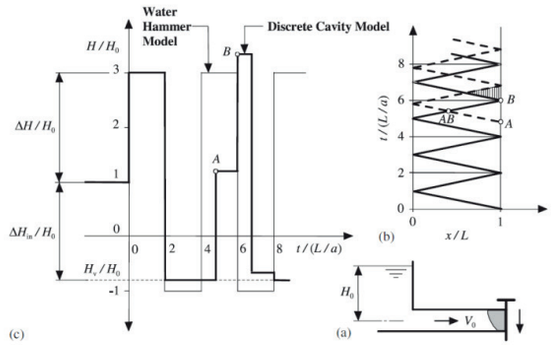

Figure 2: Formation of a short-duration pressure peak. (a) Reservoir-pipe-valve system. (b) Wave paths in distance-time plane. (c) Piezometric-head history at valve. /14/

Short-duration pressure peaks (Position B) develop, if the pressure pulse after the collapse of a cavitation zone (Position A) is superimposed by the pressure pulse of the Joukowsky impact. The resulting pressure amplitude exceeds the pressure amplitude theoretically calculated through the Joukowsky equation. The highest pressure gradients occur at the intersection of both wave fronts (Position AB).

Since no own measurement data stood at disposal to validate the water hammer simulation, the calculation results were compared with published measurements of *Bergant* /17/, who uses a test rig construction represented in **Figure 3**.

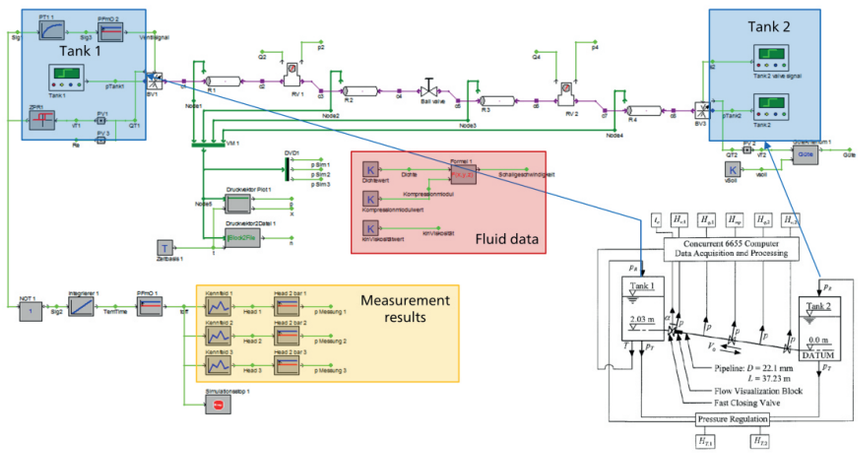

Figure 3: Simulation model of a water hammer test rig according to /17/

The test rig consists of two pressurised tanks which are connected by a copper pipe. Water hammer is initiated by a quick shut-off valve, that closes after a stationary flow situation is adjusted in the pipe.

For pressure peaks with a following cavitation **Figure 4** presents the comparison of the simulation results with the measurement results from *Bergant* /17/. The left two graphics show the pressure signals very close to the valve, the right two graphics show pressure signals in the middle of the pipe. The red curves are the digitized measuring which serves as reference curves for the blue result curves of the simulations. For a velocity of flow of 0.3 m/s, the simulated pressure pulses achieve a very good agreement with those of the measuring. Later in the simulation, the pressure remains a little too long in the cavitation, which results in a slight phase shift between simulation and measuring. In the upper left graphic, also a short-duration pressure peak, described in Figure 2, can be recognized in the simulation results.

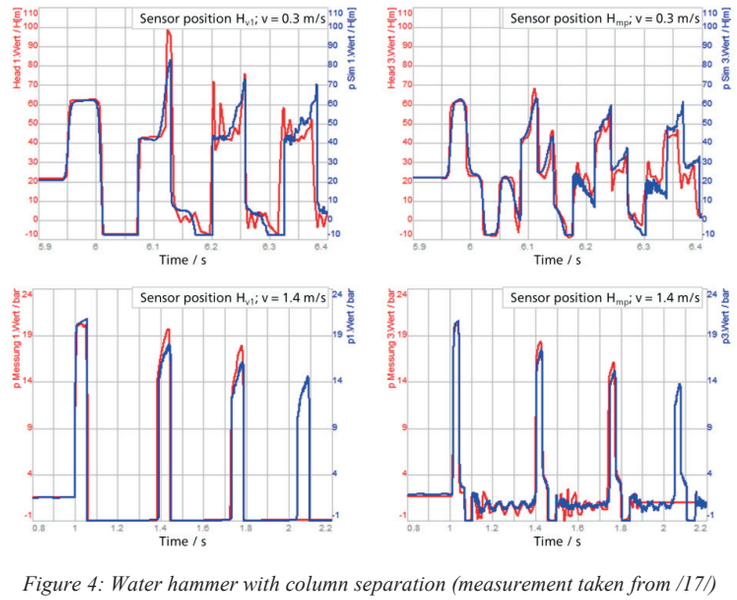

Figure 4: Water hammer with column separation (measurement taken from /17/) simulation (blue) measurement (red)

Important for the simulation of the water hammer in a tank pipe are the pressure peaks which result from the collapse of the cavitation or pseudo cavitation zone. The lower series in Figure 4 shows that at a velocity of flow of 1.4 m/s, the pressure pulses measured after the cavitation events are met very well. Even the intermediate pressure oscillations of the calculated pressure signal for the line centre fit qualitatively to the measured oscillations. In addition to this the pressure at the middle of the pipe falls only very briefly to vapor pressure level, whereas the pressure at the valve stays at vapor pressure level until the next water hammer event. Thus, it is obvious that the pipe model also covers quite well the expansion of the cavitation zone along the middle axis of the pipe. The very good qualitative agreement between simulation and measuring is now permitting to use the simulation for the calculation of the critical pressure gradients as well.

3 Water hammer simulation in return pipes

At the example of a tank pipe with a nominal diameter of 100 mm, the water hammer behaviour is calculated automatically for the influence factors velocity of flow, pipe length, braking pressure difference and valve closing time. The combination of the results of simulation to nomograms delivers in conclusion an easily understandable aid for the lay-out of a tank pipe. Critical operation points which could lead to water hammers then can already be identified at a very early project stage and can be avoided by corresponding measures without effortful changes.

The simulation model applied for the automated calculation is presented in **Figure 5**. The tank pipe which is modelled from four individual pipe pieces is central in the graphic. Every pipe is subdivided along the centre line into numerous elements that form a numerical grid. For each grid point the local pressure, the velocity of flow, the

fluid's sonic speed and the cavitation volume are calculated. These pipe internal values are summarized to vectors and stored into files so that, after the simulation, the dynamics of the water hammer can be analysed along the centre line. The other parts of the model serve for the specification of the fluid data, for the calculation of the theoretical pressure amplitude of the *Joukowsky* impact /2/ and for the calculation of the pressure gradients directly at the entrance of the pipe.

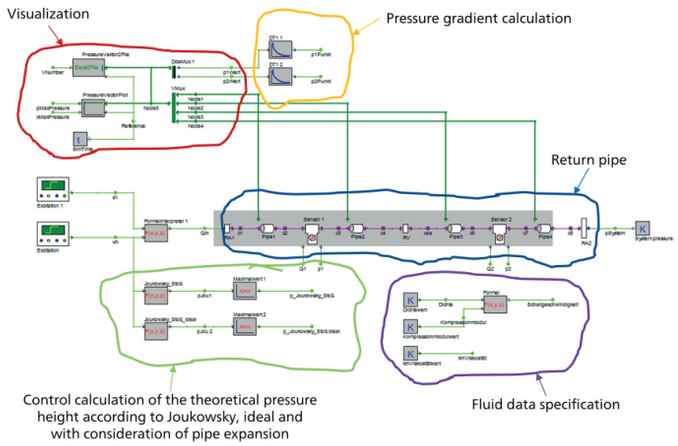

Figure 5: Simulation model, to analyse water-hammer events in return pipes

Throughout the water hammer simulation, the velocity of flow is slowly increased from 0 m/s toward the desired velocity of flow. Multiplied with the cross-sectional area of the pipe, this leads to the flow Q_{in} that is applied to the left end of the pipe. The right end of the pipe is open, and a constant braking pressure is specified. In the simulation, a braking pressure of 0 bar represents an atmospheric pressure of 1 bar absolute. In case of HFC fluid, the vapor pressure is around 80 mbar absolute and the effective braking pressure difference Δp would be 0.92 bar.

Figure 6 represents the time series results for pressure and flow of a water hammer calculation for HLP fluid directly at the beginning of the tank pipe. The amount of undissolved air considered during simulation is 0.03 %. This is, according to *Schmitz* /9/, a laboratory value that warrants a conservative estimation of pressure gradients and pressure amplitudes during the simulation study. Real values for undissolved air in hydraulic systems with mineral oil are significantly higher. It is generally valid that the smaller the amount of undissolved air is, the larger the amplitudes of the water hammer get.

Boundary conditions:
- Fluid: HLP 46, 40 °C
- Amount of undissolved air: < 0.03 %
- Pipe length: 2.5 m
- Pipe diameter: 100 mm
- Velocity of flow: 4 m/s
- Braking pressure difference: 1 bar
- Valve closing time: 50 ms

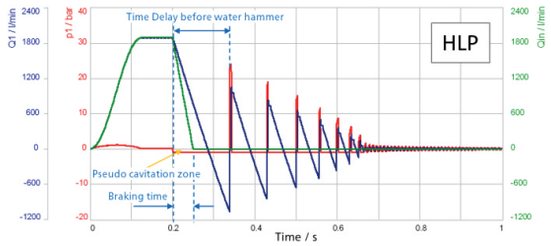

Figure 6: Water hammer calculation for a tank pipe of a hydraulic system with HLP 46

After 0.2 s the water hammer simulation reaches constant flow conditions. The flow Q_{in} (green curve) is now linearly shut-off during the valve closing time of 50 ms, what initiates the deceleration of the fluid column and because of this starts the water hammer event. It is visible that already at the start of the deceleration process at 0.2 s the flow Q_1 (blue curve) declines lower than the input flow Q_{in}. The flow balance is therefore negative, and the cavitation starts. This is also visible in the pressure signal p_1 (red curve) that falls onto vapor pressure level.

During the braking action the flow Q_1 continuously falls until it reaches zero value at approx. 0.28 s. At this point the fluid column stands still. In the further course the flow signal Q_1 becomes negative, which means that the fluid column now is running back towards the entrance of the pipe. Water hammer occurs at about 0.34 s.

As mentioned afore, the development of cavitation is strongly influenced by the presence of undissolved air which, in practice, is very difficult to measure. In case of water hammer simulation with HFC fluid (**Figure 7**) a value of 0.001 % undissolved air is selected from literature /18/ to ensure a conservative water hammer estimation. The simulation set-up is identical to that of Figure 6. However, in case of HFC the fluid column stops at about 0.32 s and the first water hammer happens at about 0.4 s and creates a clearly higher pressure amplitude than the first water hammer of the HLP system.

Boundary conditions :
- Fluid: HFC, 40 °C
- Amount of undissolved air: = 0.001 %
- Pipe length: 2.5 m
- Pipe diameter: 100 mm
- Velocity of flow: 4 m/s
- Braking pressure difference: 1 bar
- Valve closing time: 50 ms

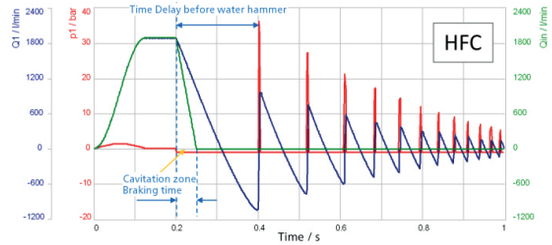

Figure 7: Water hammer calculation for a tank pipe of a hydraulic system with HFC

The simulations represented in Figure 6 and Figure 7 show that there is more than one water hammer event before the fluid column comes to a complete stop. The mechanical analogy to a spring mass system is well suitable to illustrate the causes for it. During braking the mass by the spring, kinetic energy is converted into potential energy. The mass is then accelerated by the tense spring again before the deceleration process starts once more. If this process were friction free, then an infinite sequence would be carried out of changes between kinetic and potential energy. In reality, a spring mass oscillation abates, however, since energy is permanently withdrawn from the system and changed into heat by friction. The friction in hydraulic systems has the same effect.

The stored internal pipe values enable alternative visualisations of the sequence of water hammer events. **Figure 8** presents 3D plot visualisations of the simulations of Figure 6 and Figure 7, which also include the length of the pipe. In the chosen view perspective, the time axis (blue labelled) of the 3D plots starts in the right-hand corner. The simulations end after 1 s, what is the front left-hand corner of the 3D plot. The pipe length (red labelled axis) starts with zero at the front left-hand corner, what represents the start of the tank pipe behind the shut-off valve, and increases to the pipe's outlet into the tank, that is represented by the left-hand corner in the back of the 3D plot.

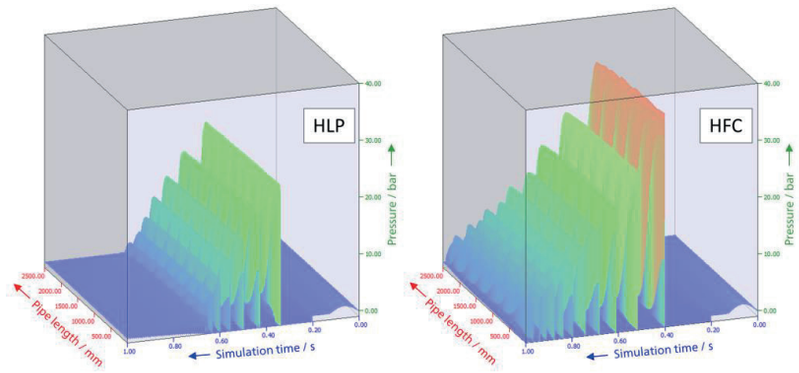

Figure 8: Pressure plots visualise the sequence of water hammer along the pipe axis

What looks like a small wave in the pressure plane (between 0 s and 0.1 s) is the pressure difference required to accelerate the fluid column at the start of the water hammer simulation. After the shut-off valve closure at 0.2 s the pressure drops down to vapor pressure and the sequence of water hammer events starts.

To analyse the dynamic situation inside the tank pipe during a water hammer event, it is helpful to visualise also the other pipe internal values (see explanation to Figure 5). In this context **Figure 9** presents top views onto 3D plots, which present the size of the cavitation zone for three different applications. The left graphic relates to the simulation presented in Figure 7. This could be an example for a tank pipe of a typical industrial hydraulic system. The middle graphic relates to a simulation with 1.0 m pipe and a velocity of flow of 14 m/s and represents a high dynamic hydraulic actuator, such as a shooting cylinder in a pressure die casting machine. The right graphic is a forecast simulation onto water hammer events in a system with a 0.25 m pipe and extremely high velocity of flow of 30 m/s.

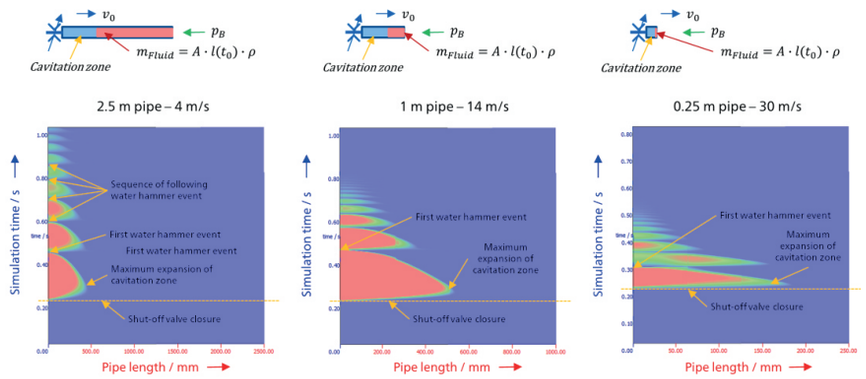

Figure 9: Size of cavitation zones during water hammer simulation

In all three cases it is obvious, that after the closure of the shut-off valve at 0.2 s cavitation zones (red area) develop. The cavitation zones expand during the deceleration of the fluid column, reach a maximum that indicates the standstill of the fluid column, and then shrink due to the returning fluid column. Once the cavitation zones are completely compressed a water hammer event takes place.

It is obvious from Figure 9 that independent of the specific setup it is not possible for the cavitation zone to expand throughout the entire pipe. The reason for this is the reduction of the moving fluid mass that is proportional to the expansion of the cavitation zone in the pipe. Through this, the braking acceleration continuously increases if the braking pressure is constant. Thus, the braking acceleration would tend against infinite, if there were almost no mass left in the pipe.

As mentioned, the simulation also considers undissolved air for the calculation of the pressure dependent fluid properties. The three graphics in Figure 10 present an overview of the speed of sound during the water hammer events of the three examples introduced in Figure 9.

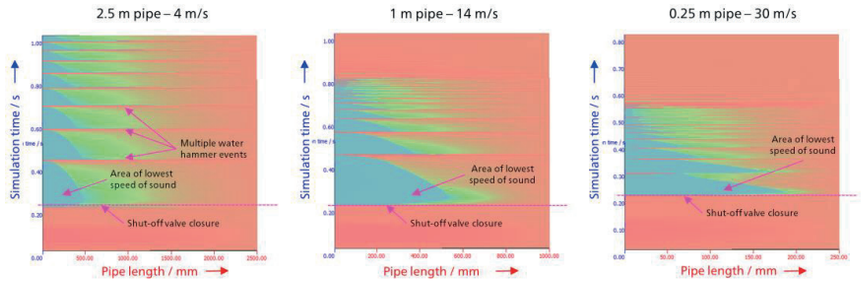

Figure 10: Speed of sound during water hammer simulation

The red coloured areas represent regions with a speed of sound according to the chosen braking pressure. The blue colour represents regions where the speed of sound corresponds to the vapor pressure level. Especially the two more dynamic examples with a velocity of flow of 14 m/s and 30 m/s have noticeably small green transition regions between the red and the blue regions. The reason for the rapid transition is the dramatic reduction of the speed of sound if at low pressure the undissolved air bubbles expand. Because of the expanding air bubbles, the fluid's air volume fraction increases, what directly leads to a reduced effective bulk modulus of the fluid and therefore also leads to the reduction of the speed of sound. At least now it becomes clear that the examination of water hammer events in tank pipe requires the usage of numerical simulation because the *Joukowsky* equation /2/ covers only water hammer at constant speed of sound.

4 Automatic water hammer analysis

The simulation results show that it is possible to determine the pressure amplitudes, the critical pressure gradients and even the duration of the pressure peaks numerically. It depends on the individual boundary conditions of the respective plant, however, under which conditions water hammers occur. Here the advantages of the numeric simulation become obvious, because by a parameter variation a broad spectrum of possible system configurations can automatically be calculated.

The automated simulation is based on the simulation model already introduced in Figure 5, that is enlarged by elements for the parameter specification and for the automatic data export (**Figure 11**).

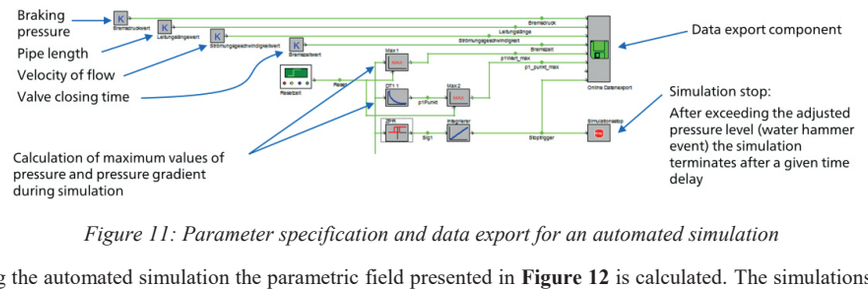

Figure 11: Parameter specification and data export for an automated simulation

During the automated simulation the parametric field presented in **Figure 12** is calculated. The simulations have been conducted with HLP fluid and HFC fluid, to enable a direct comparison of water hammer behaviour in the reference system. Each of the 17,360 simulations per fluid supplement the result file with a data line so that at the end of the simulation, all information is available on a consolidated basis. The simulations have been distributed throughout the office network, so that 5 desktop computers with together 36 cores were busy for almost 7 days.

Parameter	Pipe length	Velocity of flow	Valve closing time	Braking pressure difference
Subdevision	0.25 m to 2.5 m in 0.25 m steps	0.0 m/s to 30 m/s in 1.0 m/s steps	10 ms to 150 ms in 20 ms steps	1.0; 2.0; 3.5; 6.0; 8.5; 16.0 and 31.0 bar
Amount	10	31	8	7
Data field 1 (Braking time and breaking pressure is constant)	10 x 31 = 310 simulations		constant	constant
Data field 2 (Braking pressure is constant)	8 x Data field 1 = 2,480 simulations			constant
Data field 3	7 x Data field 2 = 17,360 simulations			

Figure 12: Parameter field of an automated water hammer analysis

For water hammer analysis the short valve closing time of 10 ms is particularly critical. For this valve closing time **Figure 13** shows exemplarily the comparison of data field 1 for the braking pressure differences 1.0, 6.0 and 16.0 bar for a system with HFC fluid. The cells where the pressure exceeds the value of 200 bar during the pressure blow are inked red. The edge of the red area therefore represents a kind of "tolerance threshold".

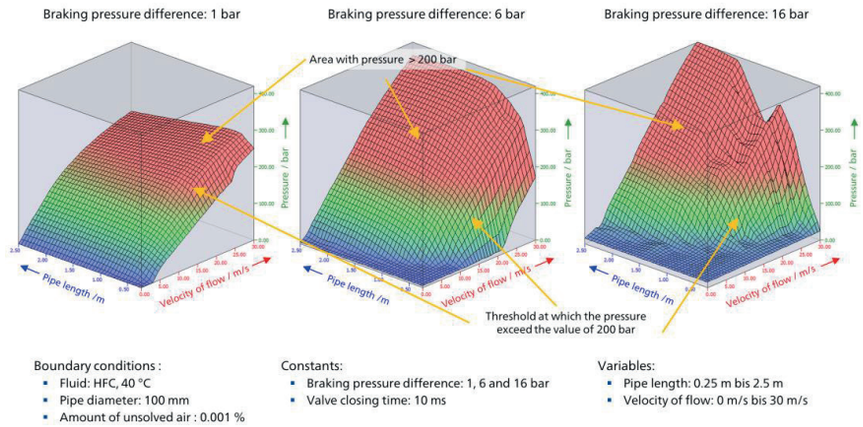

Figure 13: Variant computation at 10 ms valve closing time

Figure 13 left diagram illustrates that water hammers are unavoidable in the tank pipe at ambient pressure already at very low velocities of flow. Independent of the pipe length and for velocities of flow above 15 m/s the maximum pressure during the water hammer is higher than 200 bar. If the tank pipe is prestressed by a braking pressure of 5 bar (Figure 13, middle diagram, braking pressure difference = 6 bar), then a range without any water hammers arises for low velocities of flow and short tank lines.

This is accompanied by a rise of the maximum pressure amplitude at velocities of flow above 15 m/s and line lengths over 0.75 m, though. If the braking pressure is still further increased (Figure 13, right diagram, braking pressure difference = 16 bar), then the range without water hammers enlarges for short tank pipes up to high velocities of flow. If the length of the tank pipe increases, however, then directly water hammers develop with amplitudes from 200 bar and more.

Figure 14 shows an alternative comparison of results of the three braking pressure differences 1.0, 6.0 and 16.0 bar. This time the velocity of flow is constant 4.0 m/s and the diagrams represent an extract of data field 2. Visualised is the maximum pressure gradient during water hammer depending on pipe length (red labelled axis) and valve closing time (blue labelled axis). The cells where the pressure gradients exceed the value of 100,000 bar/s during the pressure blow are inked red. The edge of the red area therefore represents the pressure gradient threshold that was experimentally determined by *Lipphardt* /4/ to be critical for micro diesel effects in oil hydraulic systems (HLP fluid).

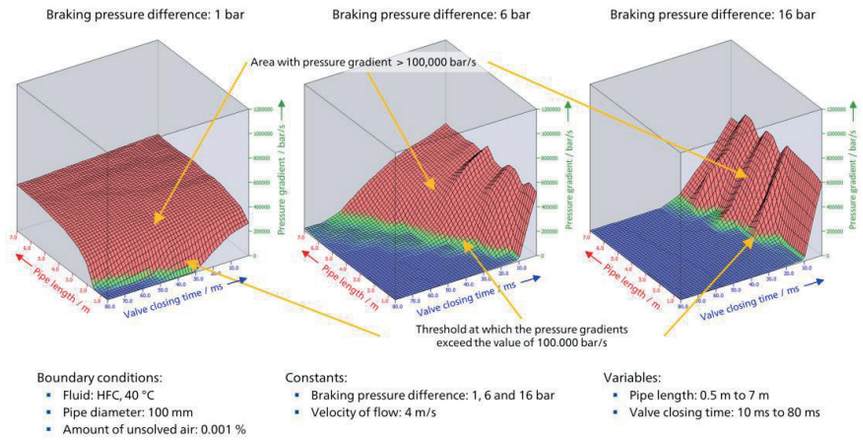

Figure 14:Variant computation at 4 m/s velocity of flow

Figure 14 left diagram indicates that, at ambient pressure, there is only a small region at low valve closing times and short pipes without water hammer and therefore almost no pressure gradients. The middle diagram shows that, for a breaking pressure difference of 6 bar, there is no critical pressure gradient for a wide range of pipe length to valve closing time combinations. This range can even be enlarged if the breaking pressure difference (Figure 14, right diagram) is further increased. However, it is also obvious from the middle and the right diagram that the threshold at which high pressure gradients will be present in case of water hammer will become more distinct with increased braking pressure. For practical application this is most interesting since it provides an explanation for the fact that many applications run without water hammer problems for a long time and suddenly are prone to water hammer events, for example after a system revision to make the hydraulic drive more dynamic.

5 Nomograms and remedial measures

For practical work the representation of the critical pressure gradients or absolute pressure amplitude heights with single diagrams is much too unhandy, because for every relevant braking pressure difference versus valve closing time or versus velocity of flow combination there must be a diagram of its own. Since this paper's focus is on the explanation of simulations, that are the foundation of a simulation-supported water hammer analysis, it is referenced to *Baum* and *Scheffel* /6, 7/ for a more widespread explanation of how exactly the nomograms are generated and how they can be interpreted.

In principle, only the threshold from which a certain pressure or a certain pressure gradient is exceeded, is interesting and the result data therefore can further be summarized. In this context, it is again pointed out that the threshold curves are application and system dependent, so that the presented nomograms must be understood as examples that show the potential of the methodology.

Figure 15 presents a comparison of critical pressure gradients in the example hydraulic system with HLP fluid and with HFC fluid. Both diagrams represent threshold curves for different braking pressure differences from which the critical value exceeds 100,000 bar/s.

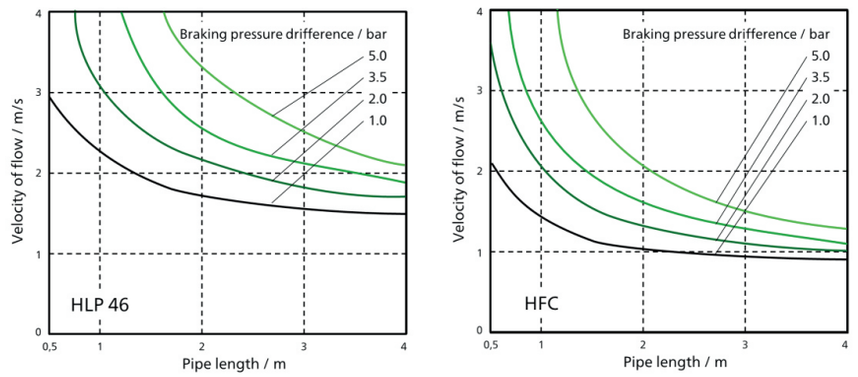

Figure 15: Comparison of critical pressure gradients in hydraulic systems with HLP and HFC fluid

The two diagrams in Figure 15 illustrate that the water hammer vulnerability of a tank pipe highly depends on the fluid properties and, in both cases, improves with the prestress pressure in the tank pipe. Technically there are multiple remedial measures available to generate higher braking pressure differences (**Figure 16**). However, the implementation of additional components into the system implies a change of the overall system's dynamic. It is therefore advisable to use the numerical simulation to crosscheck the interaction of the designed remedial measure, prior to its application in the real system.

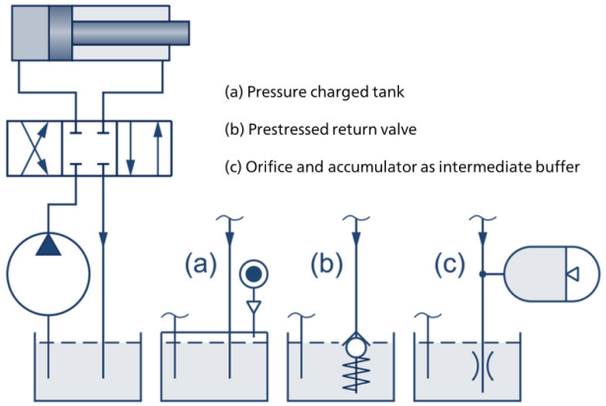

Figure 16: Remedial measures to increase the braking pressure difference

6 Summary and Conclusion

Water hammer events in tank pipes that can lead to damages to the plant by cavitation and diesel effects are not tolerable for modern dynamic hydraulic drives. To avoid such problems the design of the tank line must be incorporated with higher priority into the design of the hydraulic system.

The simulations presented in this paper show that nowadays numerical pipe models are available to calculate water hammer events even under consideration of cavitation effects. In combination with simulation tools that can automatically compute design parameter fields, all necessary tools are available to the engineer to analyse the water hammer vulnerability of the tank pipe prior to its realisation. Subsequently the simulation is also the tool of choice if remedial measures must be developed. The simulation is especially suitable to unveil unwanted side effects that may arise if the remedial measure interacts with the rest of the tank pipe system.

Nomenclature

Variable	*Description*	*Unit*
p_1	Pressure behind the shut-off valve at the start of the tank pipe	[bar]
Q_1	Flow behind the shut-off valve at the start of the tank pipe	[l/min]
Q_{in}	Flow through the shut-off valve	[l/min]
Δp	Braking pressure difference	[bar]
v	Velocity of flow	[m/s]

References

/1/ Mang, T., Dresel, W., ”Lubricants and Lubrication” Wiley-VCH Verlag GmbH & Co. KGaA; Auflage: 2 (11. Januar 2007)

/2/ Seite „Druckstoß“. In: Wikipedia, Die freie Enzyklopädie. Bearbeitungsstand: 15. August 2016, 20:53 UTC.URL: https://de.wikipedia.org/wiki/Druckstoß (Abgerufen: 30. Dezember 2016, 06:53 UTC)

/3/ Hörl, E., Parker Prädifa Video „Luft im Öl“, Expert Verlag, 1975

/4/ Lipphardt, P. „Untersuchung der Kompressionsvorgänge bei Luft-in-Öl-Dispersionen und deren Wirkung auf das Alterungsverhalten von Druckübertragungsmedien auf Mineralölba-sis“, Dissertation RWTH Aachen, 1975

/5/ Schmitz, K.; Kratschun, F., „Simulation der Dynamik einer Gasblase zur Untersuchung des Dieseleffektes in hydraulischen Systemen“, Ölhydraulik und Pneumatik 5/2016

/6/ Baum, H.; Scheffel, G.; Dieselgate im Tankrohr, O+P Fluidtechnik, 6/2017, Seite 38-49

/7/ Baum, H.; Scheffel, G.; Druckschläge im Gießaggregat von Druckgießmaschinen, Gießerei 104 08/2017, Seite 40-53

/8/ Murrenhoff, H.; „Grundlagen der Fluidtechnik, Teil 1: Hydraulik“, Umdruck zur Vorlesung, RWTH Aachen, 2012

/9/ Schmitz, K., „Eindimensionale Hydrauliksimulation mehrphasiger Fluide“, Dissertation RWTH Aachen, 2015

/10/ n. n., DSHplus – Simulationsprogramm für fluidtechnisch mechatronische Systeme, FLUIDON Gesellschaft für Fluidtechnik mbH, Aachen, 2017

/11/ Mambretti, S., „Water hammer Simulation“, Witt Press 2014, ISBN: 978-1-84564-680-6

/12/ Theissen, H., „Die Berücksichtigung instationärer Rohrströmung bei der Simulation hydraulischer Anlagen“, Dissertation IFAS, RWTH Aachen, 1984.

/13/ Müller, B., „Einsatz der Simulation zur Pulsations- und Geräuschminderung hydraulischer Anlagen“, Dissertation RWTH Aachen, 2002

/14/ Vardy, A. E., Brown, J. M. B., “Approximation of Turbulent Wall Shear Stresses in Highly Transient Pipe Flows”, Journal Of Hydraulic Engineering © ASCE / November 2007, 1219-1228

/15/ Bergant, A., Simpson, A. R., Tijsseling, A. S., “Water hammer with column separation: A historical review”, Journal of Fluids and Structures 22 (2006) 135–171

/16/ Neuhaus, T., „Mathematische Modellierung und vergleichende Untersuchungen zur Beschreibung von transienten Ein- und Mehrphasenströmungen in Rohrleitungen“, Dissertation Bio- und Chemieingenieurwesen der Universität Dortmund, 2005

/17/ Bergant, A.; Simpson, A. R., „Pipeline column separation flow regimes”, Journal of Hydraulic Engineering, 2014, 125:835-848

/18/ C. Landry, et.al., „Modeling of Unsteady Friction and Viscoelastic Damping in Piping Systems“, 2012